

Compound-Nucleus Processes for the Reaction $U^{235} + n^*$

E. R. RAE,[†] B. MARGOLIS, AND E. S. TROUBETZKOY
Columbia University, New York, New York

(Received June 16, 1958)

The neutron capture and inelastic scattering cross section of U^{235} are calculated on the basis of the statistical theory of nuclear reactions in the energy region up to 1.1 Mev. To carry out the program, one uses experimental data from the resonance region including the radiation width and the level spacing of the compound nucleus. One also makes use of the measured fission and total cross sections in the energy range considered, the spectrum of excited states of the target, and an exponential level-density law for the compound states. The agreement with experiment is good.

1. INTRODUCTION

IN a recently published paper,¹ Lane and Lynn have applied the method developed by Hauser and Feshbach,² and Margolis,³ to calculate the neutron capture and inelastic scattering cross sections for U^{238} and Th^{232} for neutron energies up to 1 Mev. The success of these calculations in explaining, in detail, the shape of the capture cross section curves suggests the application of this method to the interactions of neutrons with a fissile nucleus. Here, in addition to the radiation width, the level density law, and the levels in the residual nucleus, the average fission width must be known as a function of energy. Alternatively, the fission cross section may be taken as an experimental datum, in which event the fission width, the capture cross section, and the inelastic scattering cross sections are obtained from the calculation. The present paper describes the latter type of calculation for $U^{235} + n$ for neutrons of energy 10 to 1100 kev. The radiation width is taken from the experimental data in the resonance region, with the energy dependence suggested by Blatt and Weisskopf.⁴ The neutron widths are those of the "black nucleus" model, the nuclear radius being fitted to the total neutron cross section. The level density law for the compound nucleus is that of Lang and Le Couteur,⁵ and the level scheme for the residual nucleus is that proposed by Huizenga *et al.*⁶

The calculated values of the capture and inelastic scattering cross sections are in agreement with experiment up to a neutron energy of about 500 kev, indicating that the level scheme used for the residual nucleus is essentially correct up to about 400 kev. Deviations from experiment above 500 kev indicate the presence of further rotational bands built on intrinsic

or vibrational states in U^{235} . When suitable bands are added, a fit can be made to the capture and inelastic scattering cross sections up to 1 Mev and values of the mean fission width obtained. In this way information is obtained about the level density in the residual nucleus and also in the compound nucleus at the fission saddle point.

2. AVERAGE CROSS-SECTION CALCULATIONS

2.1 Cross-Section Formulas

The derivation of the average cross sections is discussed in references 1, 2, and 3. We can write the cross section for the formation of the compound nucleus followed by decay through channels r as follows:

$$\sigma_r = \frac{1}{2(2I+1)} \frac{\pi}{k^2} \sum_{l=0}^{\infty} T_n(l, E) \times \sum_{J=0}^{\infty} \left[\frac{\epsilon_{jI}^J (2J+1) T_r(J, E)}{\sum_r T_r(J, E) + \sum_{E', l'} \epsilon_{j'l'}^J T_n(l', E')} \right] \mathcal{R} \quad (1a)$$

for fission and capture, and

$$\sigma_{in} = \frac{1}{2(2I+1)} \frac{\pi}{k^2} \sum_{l=0}^{\infty} T_n(l, E) \times \sum_{J=0}^{\infty} \left[\frac{\epsilon_{jI}^J (2J+1) \sum_{E'', l''} \epsilon_{j'l''}^J T_n(l'', E'')}{\sum_r T_r(J, E) + \sum_{E', l'} \epsilon_{j'l'}^J T_n(l', E')} \right] \mathcal{R} \quad (1b)$$

for inelastic scattering.

In these equations k is the wave number of the incident neutron, E is the incident neutron energy, and E' the energy of the scattered neutron. I is the spin of the target nucleus, l and l' are the orbital angular momenta of the incident and scattered neutrons, and j is the channel spin, equal to $I \pm \frac{1}{2}$ except when $I=0$ in which case $j = \frac{1}{2}$. J is the spin of the compound nucleus which can have any value obtained by combining j and l . $\epsilon_{jI}^J = 2, 1, \text{ or } 0$ according as $|J-l| \leq j \leq J+l$ is satisfied for both channel spins j , one channel spin, or neither. The double primed quantities j'', l'' and E'' refer to the particular group of inelastically scattered

* This work partially supported by the U. S. Atomic Energy Commission.

[†] On leave of absence from Atomic Energy Research Establishment, Harwell, England.

¹ A. M. Lane and J. E. Lynn, Proc. Phys. Soc. (London) **A70**, 557 (1957).

² W. Hauser and H. Feshbach, Phys. Rev. **87**, 366 (1952).

³ B. Margolis, Phys. Rev. **88**, 327 (1952).

⁴ J. M. Blatt and V. F. Weisskopf, *Theoretical Nuclear Physics* (John Wiley and Sons, Inc., New York, 1952).

⁵ J. M. B. Lang and K. J. Le Couteur, Proc. Phys. Soc. (London) **A67**, 586 (1954).

⁶ Huizenga, Rao, and Engelkemeir, Phys. Rev. **107**, 319 (1957).

neutrons which are being observed.

$$T_n(l, E) = 2\pi \frac{\langle \Gamma_n(J, j, l, E) \rangle}{\langle D(J, E) \rangle},$$

and for fission and radiation channels

$$T_r(J, E) = 2\pi \frac{\langle \Gamma_r(J, E) \rangle}{\langle D(J, E) \rangle},$$

where $\Gamma_n(J, l, E)$ is the width of a level of spin J for the emission of l -wave neutrons of energy E , and $\Gamma_r(J, E)$ is the partial width of a level of spin J formed by the addition of a neutron of energy E , for decay through the channel r . $D(J, E)$ is the spacing of levels of spin J and one parity formed by neutrons of energy E .

T_n represents the neutron wave-mechanical penetrability of the nuclear surface and is taken to be independent of J and j . T_r will represent the probability of decay of the compound nucleus by γ emission and is a function of J through the J -dependence of $\langle D(J, E) \rangle$, the mean level spacing. T_f will represent the penetrability of the fission barrier. T_f is probably also J -dependent, though in the analysis which follows T_f will be taken to be independent of J .

$$\mathcal{R} = \left\langle \frac{\Gamma_n \Gamma_r}{\Gamma} \right\rangle \times \frac{\langle \Gamma \rangle}{\langle \Gamma_n \rangle \langle \Gamma_r \rangle},$$

and is present because the cross-section formulas are written as functions of the average widths rather than as the average of the functions.^{7,8}

2.2 Neutron Penetrabilities

The penetrability of the nuclear surface to neutrons was calculated in the manner described in Blatt and Weisskopf.⁴ According to the "black nucleus" model, one has

$$T_n(l, E) = 4xXv_l / [X^2 + (2xX + x^2v_l)v_l], \quad (2)$$

where $x = kR$, $X^2 = X_0^2 + x^2$, and $X_0 = 10^{13} \times (R \text{ in cm})$,

$$v_l = |x[j_l(x) + in_l(x)]|^{-2},$$

$$v_l = |(d/dx)\{x[j_l(x) + in_l(x)]\}|^2,$$

$j_l(x)$ and $n_l(x)$ being spherical Bessel and Neumann functions. The expression for T_n is seen to depend on R , the nuclear radius. The value of R used in the calcu-

⁷ The factor \mathcal{R} has been put equal to unity in all the work below. An attempt to take into account the variation of the widths was abandoned because of the prohibitive amount of work involved. We wish, however, to express our gratitude to Dr. Lawrence Dresner for computing for us a range of values of the \mathcal{R} factor.

⁸ L. Dresner, *Proceedings of the Columbia University International Conference on Neutron Interactions with Nuclei, 1957*, Columbia University Report CU-175, TID-7547 (available from Office of Technical Services, Department of Commerce, Washington, D. C.), p. 71.

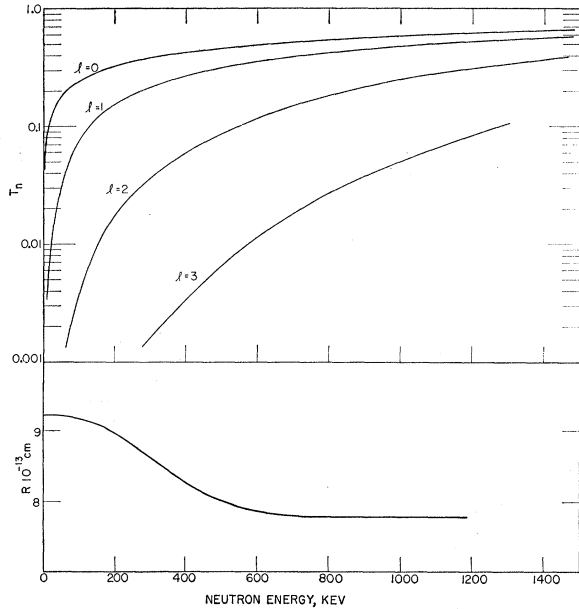


Fig. 1. Neutron penetrabilities $T_n(l, E)$ predicted by the black nucleus model with a wave number $K = 10^{13} \text{ cm}^{-1}$, and a radius shown by the lower curve. The energy dependence of the radius was obtained by fitting the experimental neutron total cross section of uranium.

lations was obtained by fitting the theoretical expression for the total cross section to the experimental results over the energy range investigated (10 to 1100 keV). R was found to vary from about 9×10^{-13} at 10 keV to 8×10^{-13} at 1100 keV so this variation was incorporated into the values of $T_n(l, E)$ used in the calculations. The penetrabilities used thus take into account, in a rough way, the giant resonance behavior of the cross section. $T_n(l, E)$ is shown for $l=0, 1, 2$, and 3 in Fig. 1, together with the variation of R with neutron energy.

2.3 Inelastic Scattering Terms

We define the inelastic scattering terms [see Eq. (1)]

$$\left. \begin{aligned} a(J) \\ b(J) \end{aligned} \right\} = \sum_{E'l'} \epsilon_{J'l'} v^J T_n(l', E'),$$

$a(J)$ and $b(J)$ being the summations for a compound-nucleus state of spin J and of odd and even parity, respectively.

To evaluate $a(J)$ and $b(J)$ it is necessary to know the level scheme for the residual nucleus. Such a scheme has been proposed by Huizenga *et al.*⁶ and is shown in Fig. 2. The levels drawn as full lines are those found experimentally and appear to belong to two rotational bands based on the $\frac{7}{2}^-$ ground state and on the $\frac{1}{2}^+$ isomeric state at 2 keV. The energies of the states belonging to the two bands can be expressed by means of the equation due to Bohr and Mottelson and given in this

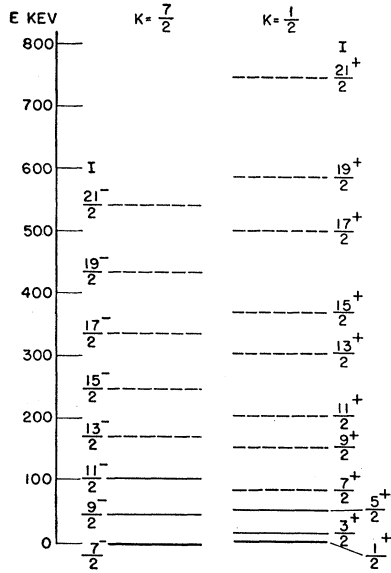


FIG. 2. Level scheme for U^{236} . Solid lines: experimentally observed levels. Dotted lines: additional levels predicted by the unified model, based on the $\frac{7}{2}^-$ ground state and on the $\frac{1}{2}^+$ isomeric state at 2 kev. In the text, reference to "experimentally observed bands" means all the levels shown here.

form by Alder *et al.*⁹:

$$E_I = E_0 + \frac{\hbar^2}{2\mathcal{I}} \{ I(I+1) + a(-1)^{I+\frac{1}{2}} (I+\frac{1}{2}) \delta(K, \frac{1}{2}) \}, \quad (3)$$

where \mathcal{I} is the effective moment of inertia of the nucleus about an axis perpendicular to the nuclear symmetry axis, and K is the projection of the total angular momentum on this axis. $\delta(K, \frac{1}{2})$ is unity for $K = \frac{1}{2}$ and zero for all other values of K , and a is a parameter which is determined from the experimental spectrum. The levels shown dotted in Fig. 2 were calculated from this formula. The values of $a(J)$ and $b(J)$ were obtained from the level scheme in Fig. 2.

2.4 Radiation Term

In calculating the radiation term $T_\gamma(J)$ we must first assume a form for the variation in the mean level spacing $D(J, E)$ with the neutron energy and the spin of the compound nucleus. We have followed Lang and Le Couteur⁵ in assuming for the compound nucleus U^{236}

$$D(J, E) = C(2J+1)^{-1} \exp[(J+\frac{1}{2})^2/35] (U+0.5)^2 \times \exp\{-[(86U)^{\frac{1}{2}} + (0.28U)^{\frac{1}{2}}]\}, \quad (4)$$

where U is the excitation of the compound nucleus in Mev, and C is a constant determined by the observed level spacing in the resonance region.

In evaluating the energy dependence of the radiation width we apply the formula⁴:

$$\Gamma_\gamma(E) \propto D(E+B_n) \int_0^{E+B_n} \frac{\epsilon^3}{D(E+B_n-\epsilon)} d\epsilon, \quad (5)$$

where B_n is the binding energy of a neutron in the com-

⁹ Alder, Bohr, Huus, Mottelson, and Winther, *Revs. Modern Phys.* **28**, 525 (1956).

pound nucleus, E is the neutron energy, and ϵ is the energy of the first γ -ray emitted by the excited compound nucleus. This formula indicates that $\Gamma_\gamma(E)$ increases monotonically with E . With the aid of Eqs. (4) and (5), $T_\gamma(J, E)$ is determined.

We must now distinguish carefully between the radiation term $T_\gamma(J, E)$ which appears in the denominator of Eqs. (1a) and (1b) and represents the competition due to all exit channels in which the compound nucleus initially emits a γ ray, and the capture term $T_c(j, E)$ which appears in the numerator of the Eq. (1a) when the capture cross section is being evaluated. In computing $T_c(J, E)$ we follow Lane and Lynn¹ and write $T_c(J, E) = 2\pi\Gamma_c(E)/D(J, E)$, where

$$\Gamma_c(E) \propto D(E+B_n) \int_E^{E+B_n} \frac{\epsilon^3}{D(E+B_n-\epsilon)} d\epsilon. \quad (6)$$

Here the limits of the integral have been changed to omit the cases where the initial γ ray has an energy less

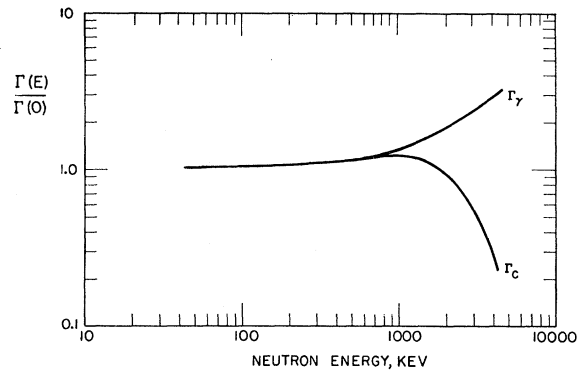


FIG. 3. Energy dependence of the capture width and of the radiation width computed as explained in the text.

than the incident neutron energy, because in these cases the initial γ ray will be almost always followed by fission or neutron emission rather than capture. When the integral in Eq. (6) is evaluated putting $B_n = 6.4$ Mev and using an appropriate level spacing law, $\Gamma_c(E)$ is found to have the energy dependence shown in Fig. 3. The interesting fact emerges that although $\Gamma_c(E)$ initially increases slowly with E as remarked by Lane and Lynn, this increase is followed by a flattening off around 1 Mev and a subsequent rapid drop. $\Gamma_\gamma(E)$ is also shown for comparison. [$D(U)$ in this calculation is approximated by $\exp\{-(aU)^{\frac{1}{2}}\}$, the value of a being adjusted to give a close approximation to Eq. (4) over the energy range of interest.]

2.5 Evaluation of the Average Cross Sections

In principle, any partial cross section can now be evaluated by substituting for all values of T_r and T_n in Eqs. (1) and summing over all l values from 0 to ∞ . In practice, it was found to be sufficient in the energy

range studied to take only $l=0, 1, 2,$ and 3 . Even so, the computational effort involved in evaluating a large number of cross section curves is considerable. A program was therefore set up for the IBM-650 computing machine, to evaluate the right-hand side of Eqs. (1). This program was used in all the work described below.

3. COMPARISON WITH EXPERIMENT

3.1 Fission Cross Section

The computer program was first used to evaluate the fission cross section for a range of values of T_f (T_f being taken to be independent of J) between 0.1 and 25. The curves obtained are shown in Fig. 4 together with an experimental curve which is based on the data compiled by Hughes and Harvey¹⁰ and on newer information due to Allen and Ferguson.¹¹ The points of intersection of the calculated curves with the experimental curve determine T_f as a function of energy.

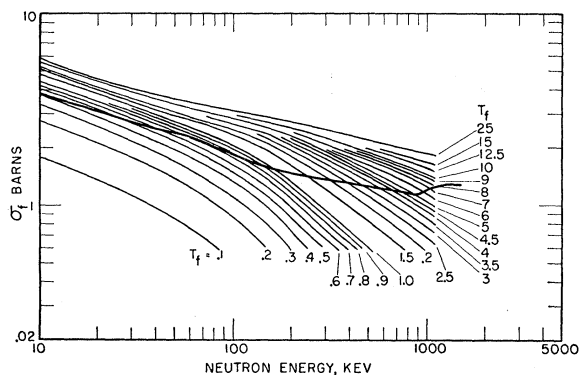


FIG. 4. Fission cross section of U^{235} . The thin lines are calculations using constant T_f . The thick line represents the experimental data.

The form of this function is shown in the full curve in the lower part of Fig. 5.

3.2 Capture Cross Section

If T_c is substituted for T_r in Eq. (1a), the capture cross section is obtained, T_f being taken from Fig. 5. The full curve in Fig. 5 then leads to the full curve in Fig. 6 which shows the variation with energy of the capture cross section.

The experimental points shown in Fig. 6 are taken from the tabulation of values of α ($\sigma_{\text{capture}}/\sigma_{\text{fission}}$) given by Oleksa,¹² coming from earlier American and Russian work,^{13,14} and from the recent measurements of α

¹⁰ Hughes and Harvey, Brookhaven National Laboratories Rept. No. 325.

¹¹ W. D. Allen and A. T. G. Ferguson, Proc. Phys. Soc. (London) **A70**, 573 (1957).

¹² S. Oleksa, J. Nuclear Engr. **5**, 16 (1957).

¹³ Kanne, Stewart, and White, *Proceedings of the International Conference on the Peaceful Uses of Atomic Energy, Geneva, 1955* (United Nations, New York, 1956), Vol. 8, p. 595.

¹⁴ I. V. Kurchatov, Nuclear Engr. **1**, 101 (1956).

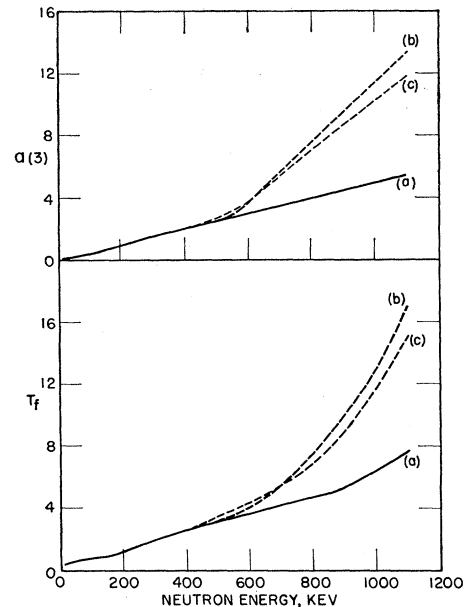


FIG. 5. The lower graph shows the variation of T_f with energy. The solid curve (a) assumes only the experimentally observed bands of the target nucleus. The dashed lines (b) and (c) in the higher energy region were obtained by assuming energy level bands above 500 keV in addition to the bands shown in Fig. 2, as explained in the text. The upper set of curves shows the energy variation of $a(3)$, a typical sum of the inelastic penetrabilities $T_n(V, E')$. The labels (a), (b), and (c) correspond to the different assumptions about the energy level spectrum of the target nucleus.

reported by Diven and Terrell.¹⁵ In all cases σ_c is obtained from α by multiplying by the appropriate value of σ_f from Fig. 4. The full curve, based on the experimentally observed rotational bands, agrees with

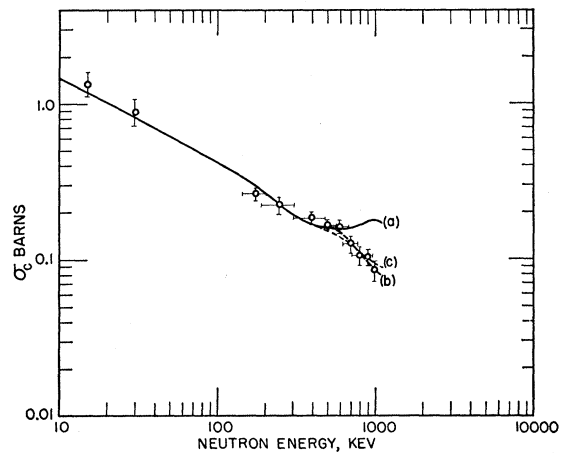


FIG. 6. Neutron capture cross section of U^{235} . The solid line (a) is the theoretical calculation based on the level scheme of Fig. 2. The dashed curves (b) and (c) are obtained by assuming energy level bands above 500 keV in addition to the experimentally observed ones, as explained in the text. The circles represent the experimental data.

¹⁵ Diven, Terrell, and Hemmendinger, Phys. Rev. **109**, 144 (1958).

TABLE I. Partial inelastic cross sections.

E (keV)	σ (barns)					
	$60 \leq Q < 350$ keV		$150 \leq Q < 500$ keV		$500 \leq Q < 750$ keV	
	Experi- mental	Calc. ($60 \leq Q$)	Experi- mental	Calc.	Experi- mental	Calc.
550	0.56	(a) 0.50 (b) 0.51 (c) 0.54				
1000			0.33	(a) 0.33 (b) 0.15 (c) 0.25	0.33	(a) 0.0011 (b) 0.50 (c) 0.38

experiment up to a neutron energy of 500 or 600 keV. Above this energy, this simple calculation predicts a slight rise in the capture cross section, contrary to experiment. By inserting into the calculation several more rotational bands based on intrinsic or vibrational levels at 500 or 600 keV, it is possible to cause the calculated curve to follow the experimental points as shown by the dotted curves. The position and number of these extra bands are not known and one has some leeway in choosing them to fit the capture cross section. The parity of a band is found to have no appreciable effect on the cross section, and the spin very little provided it is not very high. The position and number of the bands, however, do affect the capture cross section. In addition, they affect profoundly the distribution of the inelastically scattered neutrons in energy, concerning which there are some experimental data.¹⁶

3.3 Inelastic Scattering

By substituting the appropriate summation of values of $T_n(l'', E'')$ in Eq. (1b), the cross section for inelastic scattering can be computed for neutrons which leave the residual nucleus in excited states between any arbitrary energy limits (i.e., for different ranges of Q values for the reaction). Cranberg¹⁶ has given values for these partial inelastic cross sections which are compared with the calculated values in Table I.

The calculated values marked (a), (b), and (c) are obtained from the following level schemes: (a) Experimentally observed bands only. (b) Experimentally observed bands together with one band based on a $\frac{3}{2}^-$ level at 500 keV and four bands based on $\frac{3}{2}^-$ levels at 600 keV. The moment of inertia (\mathcal{J}) chosen for these bands was arbitrarily fixed between the observed values for the $\frac{1}{2}^+$ and $\frac{7}{2}^-$ bands. (c) Experimentally observed bands together with one band based on a $\frac{5}{2}^-$ level at 430 keV and three bands based on $\frac{3}{2}^-$ level at 600 keV. Assumptions (b) and (c) both lead to reasonably good agreement with the experimental capture cross section curve, but (c) leads to much better agreement with the partial inelastic cross sections at 1 Mev, thereby suggesting that the level at 400–450 keV in U^{235} is not a

¹⁶ L. Cranberg, *Proceedings of the Columbia University International Conference on Neutron Interactions with Nuclei, 1957*, Columbia University Report CU-175, TID-7547 (Available from Office of Technical Services, Department of Commerce, Washington, D. C.), p. 218.

completely arbitrary choice. The variation of the partial inelastic cross sections with energy is shown in Fig. 7.

4. DISCUSSION

It will be observed that a knowledge of the experimental low-energy level scheme for U^{235} , together with the fission cross section, enables us to calculate the absolute values of σ_c and $\sigma_{\text{inelastic}}$ up to 500 or 600 keV in good agreement with experiment. This gives us some confidence in believing the calculated curve for T_f . By inserting a rotational band based on an (arbitrary) $\frac{5}{2}^-$ level between 400 and 450 keV and three more bands based on (arbitrary) $\frac{3}{2}^-$ levels at 600 keV, we achieve simultaneously a tolerable fit to the capture and inelastic data from 500 to 1000 keV, and obtain an extension of the T_f curve to this energy. Thus the good fits obtained by Lane and Lynn to the observed capture cross sections of the two nonfissile isotopes U^{238} and

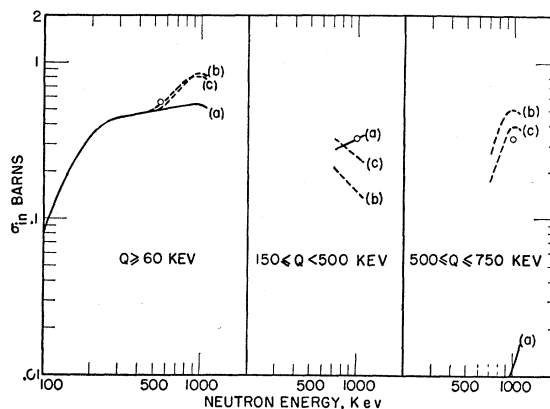


Fig. 7. Partial inelastic scattering cross section for excitation energies as indicated in the figure. The solid curve (a) was obtained by assuming only the experimentally observed bands of the target nucleus. The dashed curves (b) and (c) assume additional bands above 500 keV.

Th^{232} have been extended to the fissile isotope U^{235} where in addition to the capture and inelastic scattering cross sections we also compute the average penetrability, T_f , of the fission barrier. This parameter tells us, in fact, a mean density of levels of one spin and parity in the compound nucleus at the top of the fission barrier.^{17,18} Averaged over the energy region 0–1100 keV, there appear to be about 12 levels of any one spin and parity per Mev. It is interesting to compare the variation with energy of this level density (in the even-even compound nucleus at the top of the fission barrier) with a corresponding variation in the level density of the even-odd target and residual nucleus. The upper set of curves in Fig. 5 shows, for comparison with T_f , the variation with energy of $a(3)$, a typical sum of the in-

¹⁷ A. Bohr, *Proceedings of the International Conference on the Peaceful Uses of Atomic Energy, Geneva, 1955* (United Nations, New York, 1956), Vol. 2, p. 151.

¹⁸ J. A. Wheeler, *Physica* 22, 1103 (1956).

elastic penetrabilities $T_n(U, E')$. This represents, in the high-energy limit, the number of levels of both parities, and all spins, lying below an excitation energy equal to the incident neutron energy. It will be observed that this quantity varies with energy in a manner very similar to T_f . This similarity of behavior with energy of T_f and $a(J)$ must also persist at higher energies since, as has been remarked by Huizenga,¹⁹ the fission cross section is normally constant over a neutron energy range of 2–5 Mev. This constancy indicates a

¹⁹ J. R. Huizenga, Phys. Rev. **109**, 484 (1958).

constant division of the available cross section between fission and inelastic scattering, and hence a similar behavior of the two corresponding level densities with energy.

ACKNOWLEDGMENTS

We would like to express our gratitude to Miss Sophie Oleksa for several helpful discussions of the work. We also wish to thank the Watson Laboratories of the International Business Machines Corporation for the use of their computing facilities.

Some Measurements of Atmospheric Neutrons*†

JOHN D. GABBE‡

Physics Department, New York University, University Heights, New York

(Received March 4, 1958; revised manuscript received July 17, 1958)

A series of airplane flights carrying neutron counters to an altitude of 700 g cm⁻² was made at 52°20' north geomagnetic latitude in 1955. Enriched and normal BF₃ counters were covered with Cd, Sn, Pyrex, and lime-glass shields. The ratios of the counting rates of the variously shielded counters are compared with the ratios calculated theoretically on a thick-shield basis using the neutron energy distribution function derived by Freese and Meyer. The neutron-production data taken by Davis and by Staker with Pyrex-glass-envelope BF₃ counters are corrected for the absorption of neutrons by the boron in the Pyrex. The corrected neutron-production rates are recalculated to be 2.1±0.4 cm⁻² sec⁻¹ and 0.9±0.2 cm⁻² sec⁻¹ at 54°36' and 30°24' north geomagnetic latitude, respectively, using recent values for the various neutron cross sections. These corrected rates agree, to within 5%, with the recent measurements reported by Soberman. The above energy distribution function was found, within the limited accuracy of the experiment, to describe the energy distribution of atmospheric neutrons.

INTRODUCTION

IT is generally accepted, at present, that almost all of the neutrons in the atmosphere are secondary particles produced by the events generated when primary cosmic rays impinge on the atmosphere.^{1,2} Davis,³ Staker,⁴ and many other investigators⁵ have concerned themselves with the processes in which these neutrons are produced and absorbed. A recent calculation of the energy spectrum of a portion of the neutrons in the atmosphere was made by Freese and Meyer.¹ The neutrons treated by Freese and Meyer¹ will be referred to as *lambda* neutrons. Lambda neutrons

comprise atmospheric neutrons having energies less than E_0 , where E_0 lies between 10 kev and 0.1 Mev.

The purposes of this experiment were (1) to obtain further experimental information on the energy spectrum of lambda neutrons in that portion of the atmosphere in which the neutron density varies exponentially with pressure altitude; and (2) to correct the measurements of Davis³ and of Staker⁴ for the effect of the B¹⁰ in the Pyrex-glass envelopes of the boron-trifluoride neutron counters they used, and by using more recent information on neutron cross sections bring their calculations up to date.

The region of the atmosphere in which the neutron density varies exponentially with pressure altitude (namely, the region between an altitude of about 200 g cm⁻² and an altitude H , where H is not more than about 750 g cm⁻² and is at least 100 g cm⁻² above the ground⁶⁻⁸) will be referred to as the equilibrium region of the atmosphere. More than 90% of the neutrons in the atmosphere originate in evaporation stars.^{1,2,6,9} Theoretically one would expect no variation in the

* An abridgment of a dissertation submitted to the Graduate School of Arts and Science in partial fulfillment of the requirements for the degree of Doctor of Philosophy at New York University.

† The work herein reported was supported by a joint program of the U. S. Atomic Energy Commission and the Office of Naval Research.

‡ Present Address: Bell Telephone Laboratories, Incorporated, New York, New York.

¹ E. Freese and P. Meyer, "Neutronen in der Atmosphäre," in *Kosmische Strahlung*, edited by W. Heisenberg (Springer-Verlag, Berlin, 1953), second edition.

² J. A. Simpson, Jr., Phys. Rev. **83**, 1175 (1951).

³ W. O. Davis, Phys. Rev. **80**, 150 (1950).

⁴ W. P. Staker, Phys. Rev. **80**, 52 (1950).

⁵ Bibliographies may be found in references 1, 8, and 16.

⁶ Bethe, Korff, and Placzek, Phys. Rev. **57**, 573 (1940).

⁷ L. C. L. Yuan, Phys. Rev. **81**, 175 (1951).

⁸ R. K. Soberman, Phys. Rev. **102**, 1399 (1956).

⁹ Simpson, Fonger, and Treiman, Phys. Rev. **90**, 934 (1953).